Temporal evolution of mesoscopic structure and dynamical scaling of the structure factor of some non-Euclidean systems

S. Mazumder,* D. Sen, and A. K. Patra
Solid State Physics Division, Bhabha Atomic Research Centre, Mumbai 400 085, India

S. A. Khadilkar and R. M. Cursetji
Research and Consultancy Directorate, R & D Division, The Associated Cement Companies Limited, Thane 400 604, India

R. Loidl, M. Baron, and H. Rauch
Atominstitut der Osterreichischen Universitaten, A-1020 Wien, Austria

(Received 24 February 2005; revised manuscript received 20 September 2005; published 30 December 2005)

Real time kinetics of hydration of calcium silicates with light and heavy water has been investigated at the mesoscopic length scale with the ultra small-angle neutron scattering technique. The scattering data could not be interpreted in terms of a linear theory of phase formation. The predictions of nonlinear theories on the dynamics of phase formation have been examined. The validity of the dynamical scaling hypothesis for phase formation has also been explored. For the real time hydration of silicates with light water, reasonable agreement has been observed with a dynamical scaling hypothesis with a different measure of the characteristic length. The temporal evolution of the characteristic length does not follow a power-law relation with time. It increases with time and reaches a plateau. The mesoscopic structure of the hydrating pastes could not be described in terms of a classical porous medium with a well-defined specific inner surface. In the case of hydration with light water, the hydrating mass exhibits a mass fractal nature throughout hydration, with the mass fractal dimension increasing with time and reaching a plateau. But, in the case of hydration with heavy water, no agreement has been observed with the scaling hypothesis. For hydration with heavy water, the microstructure of the hydrating mass undergoes a transition from mass fractal to surface fractal and subsequently to mass fractal. The qualitative and quantitative features of the kinetics of hydration, as measured in scattering experiments, are strikingly different for hydration with light and heavy water.

DOI: 10.1103/PhysRevB.72.224208 PACS number(s): 64.75.+g, 61.43.Hv, 61.50.Ks

I. INTRODUCTION

For several years now, there has been strong interest in the phenomenon of dynamics of phase formation in condensed systems of broken symmetry quenched from a continuous-symmetry phase. Broken-symmetry phases are the topological defects in an otherwise homogeneous medium of continuous symmetry. The field has been receiving considerable experimental attention due to the relevance of this phenomenon in a wide range of materials including metallic alloys,[1–12] polymers,[13–18] glasses,[19–29] liquid mixtures,[30–36] binary gases,[37] ceramics,[38–40] and xerogels.[41] The field has received significant advancement by numerous theoretical and computational contributions.[42–47] The very early stage of this phenomenon can be rigorously described by a linear theory,[48] based on the diffusion equation. The linear theory implies that the Fourier amplitude $A(\mathbf{q},t)$ of the composition modulation $C(\mathbf{r},t)$ follows a linear temporal relation

$$\frac{dA(\mathbf{q},t)}{dt} \propto A(\mathbf{q},t) \quad \text{or} \quad \frac{dA(\mathbf{q},t)}{dt} = \alpha(\mathbf{q})A(\mathbf{q},t) \qquad (1)$$

where $\alpha(\mathbf{q})$ is the time- t-independent proportionality constant; $\mathbf{r}$ denotes the spatial coordinate of the system with $|\mathbf{r}|=r$; $\mathbf{q}$ is the scattering vector with modulus $|\mathbf{q}|=q$. Accordingly, the time-dependent structure factor $S(\mathbf{q},t)$ should exhibit exponential growth:

$$S(\mathbf{q},t) = S(\mathbf{q},0)\exp[2\alpha(\mathbf{q})t]. \qquad (2)$$

In its generality, the phenomenon of phase formation is a representative example of a first-order transition. It is also fundamental and of immense interest as an example of a highly nonlinear process far from equilibrium. The second phase grows with time and in late stages all domain sizes are much larger than all microscopic lengths. Most commonly in the limit $t \to \infty$, phase-forming systems exhibit a self-similar growth pattern with dilation symmetry and a scaling phenomenon,[47] i.e., the morphological pattern of the domains at earlier times looks statistically similar to the pattern at later times apart from the global change of scale implied by the growth of the characteristic length scale $L(t)$—a measure of the time-dependent domain size of the new phase. The scaling hypothesis assumes the existence of a single characteristic length scale $L(t)$ such that the domain sizes and their spatial correlation are time invariant when lengths are scaled by $L(t)$. Quantitatively, for isotropic systems, the equal-time spatiotemporal composition modulation autocorrelation function $g(r,t)$, reflecting the way in which the mean density of the medium varies as a function of r from a given point, should exhibit a scaling form with time-dependent dilation symmetry:

$$g(r,t) = f(r/L(t)). \qquad (3)$$

The scaling function $f(r/L(t))$ is universal in the sense that it is independent of initial conditions and also of interactions as

long as they are short ranged.[49] However, the form of $f(r/L(t))$ depends nontrivially on n, the number of components in the vector order-parameter field exhibiting the scaling behavior, and d, the dimensionality of the system. It is important to note that the scaling hypothesis has not been proved conclusively except for some model systems.[47] The Fourier transform of $g(r,t)$, the structure factor or scattering function $S(q,t)$ for a d-dimensional system, obeys the simple scaling ansatz[47] at late times,

$$S(q,t) = [L(t)]^d F(qL(t)). \tag{4}$$

For a phase-forming system with a nonconserved n-component vector order parameter field, the scaling function $F(qL(t))$ in Fourier space in the domain of large q $[qL(t) \gg 1]$ asymptotically approaches the form

$$F(x) \sim x^{-(d+n)}. \tag{5}$$

It is noteworthy that the Porod law, applied for systems with scalar order parameter and recognized as arising from defect configurations with sharp domain walls, $S(q) \sim q^{-4}$, is recovered from the asymptotic relation as the special case for $d=3$ and $n=1$ (scalar field). For $n=d$, the topological defects are point defects. For $n<d$, the defects are spatially extended, where the field of the order parameter varies only in n dimensions orthogonal to the defect core and is uniform in the remaining $d-n$ dimensions parallel to the core. The domain walls are the surfaces of dimension $d-n$. For $n=1$, the defects are interfaces or domain boundaries. For $n=2$, the defects are vortices and antivortices and for $n=3$, the defects are monopoles. There exist substantial differences between the $n=1$ and $n>1$ cases. For $n=1$, the interfaces are sharp, while for $n>1$, the interfaces are smooth because of the symmetry obeyed by the order parameter.

For systems where the new phase is polydisperse in nature, there is no universal form for $L(t)$. In cases[3,5,12,24,25,41] where a scaling phenomenon has been observed, $L(t)$ has been taken to be the reciprocal of the first moment of $S(q,t)$ in q space, i.e.,

$$L(t) = \left(\int qS(q,t)dq \right)^{-1}. \tag{6}$$

In some other cases,[50–52] the phenomenon has been observed where $L(t)=[q_m(t)]^{-1}$ and $q_m(t)$ is the value of q at which $S(q,t)$ has its maximum. For a model system where the free-energy functional is invariant under global rotation of the order parameter, defined by an n-component vector field, with $n=\infty$ and arbitrary d, it is found[53] that the scaling ansatz (4) breaks down because of the existence of two marginally different length scales—$L(t) \sim t^{1/4}$ and $[q_m(t)]^{-1} \sim [t/\ln(t)]^{1/4}$. In the scaling regime $L(t) \sim t^{\beta}$, where β depends on the conservation laws governing the dynamics and the dimensions[54] of n and d.

Investigations on scaling phenomena have been carried out for Euclidean systems having three[3,5,12,24,25,41,50–52] and two[55] dimensions. Investigations have been carried out also for systems having a new phase for which the number of components of the order parameter, $n \leqslant d$, the spatial dimension. The phenomenon has been investigated even for multicomponent alloys.[10–12] The validity of the scaling laws for some systems that do not support stable topological defects, having $n>d$, like liquid crystals with complicated order parameter,[56–58] has been established. The question arises about the validity of the scaling laws for phase formation in the case of non-Euclidean fractal systems. The present investigation is a step in that direction. The present work is a report of an investigation on structure factor scaling in hydrating systems.

In this work, real time hydration of tricalcium silicate ($3CaO \cdot SiO_2 \equiv C_3S$), dicalcium silicate ($2CaO \cdot SiO_2 \equiv C_2S$), and anhydrous ordinary portland cement is investigated. Tricalcium silicate and dicalcium silicate are the two major components of ordinary portland cement (OPC). OPC is actually a mixture of several calcium silicate and calcium aluminate phases. The hydration reactions of C_3S and C_2S can be written as

$$3CaO \cdot SiO_2 + (3+y-x)H_2O \rightarrow (CaO)_x(SiO_2) \cdot (H_2O)_y + (3-x)Ca(OH)_2 \tag{7}$$

and

$$2CaO \cdot SiO_2 + (2+y-x)H_2O \rightarrow (CaO)_x(SiO_2) \cdot (H_2O)_y + (2-x)Ca(OH)_2, \tag{8}$$

respectively.

In the above reactions, both x and y vary. The product $(CaO)_x(SiO_2) \cdot (H_2O)_y$ is calcium silicate hydrate, a colloidal gel-like material having very low crystallinity, usually abbreviated as C-S-H in cement literature. The hyphens in C-S-H indicate variable stoichiometry. The other product is crystalline calcium hydroxide $Ca(OH)_2$, usually abbreviated as CH. The gel fills much space around and between the cement particles. Because of the gel properties of C-S-H, the hydrated cement products are isotropic in nature and so is the scattering function $S(q,t)$, unlike in many crystalline systems. The isotropic nature of $S(q,t)$ of hydrated cement specimens was an important consideration in the choice of sample in the present experiment.

II. EXPERIMENT

The calcium silicates were fired, ground, and refired until only pure silicate phases were detectable with x-ray diffraction XRD. The chemical composition of the OPC used for the present experimentation is shown in Table I. Pure powder specimens of calcium silicates and OPC were mixed with heavy water (D_2O) and double-distilled light water (H_2O) at varying water/cement ratio (w/c), ranging by mass from 0.3 to 0.5 to obtain a pastelike mass. For scattering measurements approximately 0.08 ml of the freshly prepared paste was spread in a circular hole of diameter 10 mm punched on a cadmium sheet of thickness nearly 1.0 mm. The counting time of one complete scattering curve was about 6 min for real time measurements on hydrating samples varying with w/c ratio.

It has been established in the literature[38–40] that C-S-H gel has a fractal microstructure on the length scale of 1–100 nm.

TABLE I. Composition for OPC-53 grade specimen.

Oxide	%
SiO_2	21.2
Al_2O_3	4.4
Fe_2O_3	4.0
CaO	64.5
MgO	1.0
LoI	2.0
Na_2O	0.1
K_2O	0.4
TiO_2	0.07
SO_3	2.3
Industrial residue	0.7

A preliminary measurement carried out with a medium-resolution small-angle neutron scattering (SANS) facility,[59] based on nondispersive $(1,-1)$ setting of 111 reflection of silicon single crystals with sample between the two crystals, indicated the possibility of existence of inhomogeneities larger than 100 nm. So SANS measurements were carried out at the ultra small-angle neutron scattering instrument[60] S18, based on two triple-bounce channel-cut silicon crystals, at the 58 MW high-flux reactor at the Institute Laue-Langevin in Grenoble, France. The neutron flux density at the sample position of this Bonse-Hart-type[61] camera is about $10^4\ n/(\mathrm{cm}^2\,\mathrm{s})$ and the signal-to-noise ratio is better than 10^5. The wavelength λ of probing neutrons used is 1.87 Å. The scattered intensities were recorded as a function of $q[=4\pi(\sin\theta)/\lambda$, 2θ being the scattering angle]. The scattering data were corrected for background and primary beam geometry.

III. DATA INTERPRETATION AND DISCUSSION

Figure 1 depicts the time evolution of the structure factor $S(q,t)$ in absolute scale for light water hydrating calcium trisilicate, calcium disilicate, and OPC with varying w/c ranging from 0.3 to 0.5, respectively. It is evident from Fig. 1 that with increasing hydration time, the curvature of the

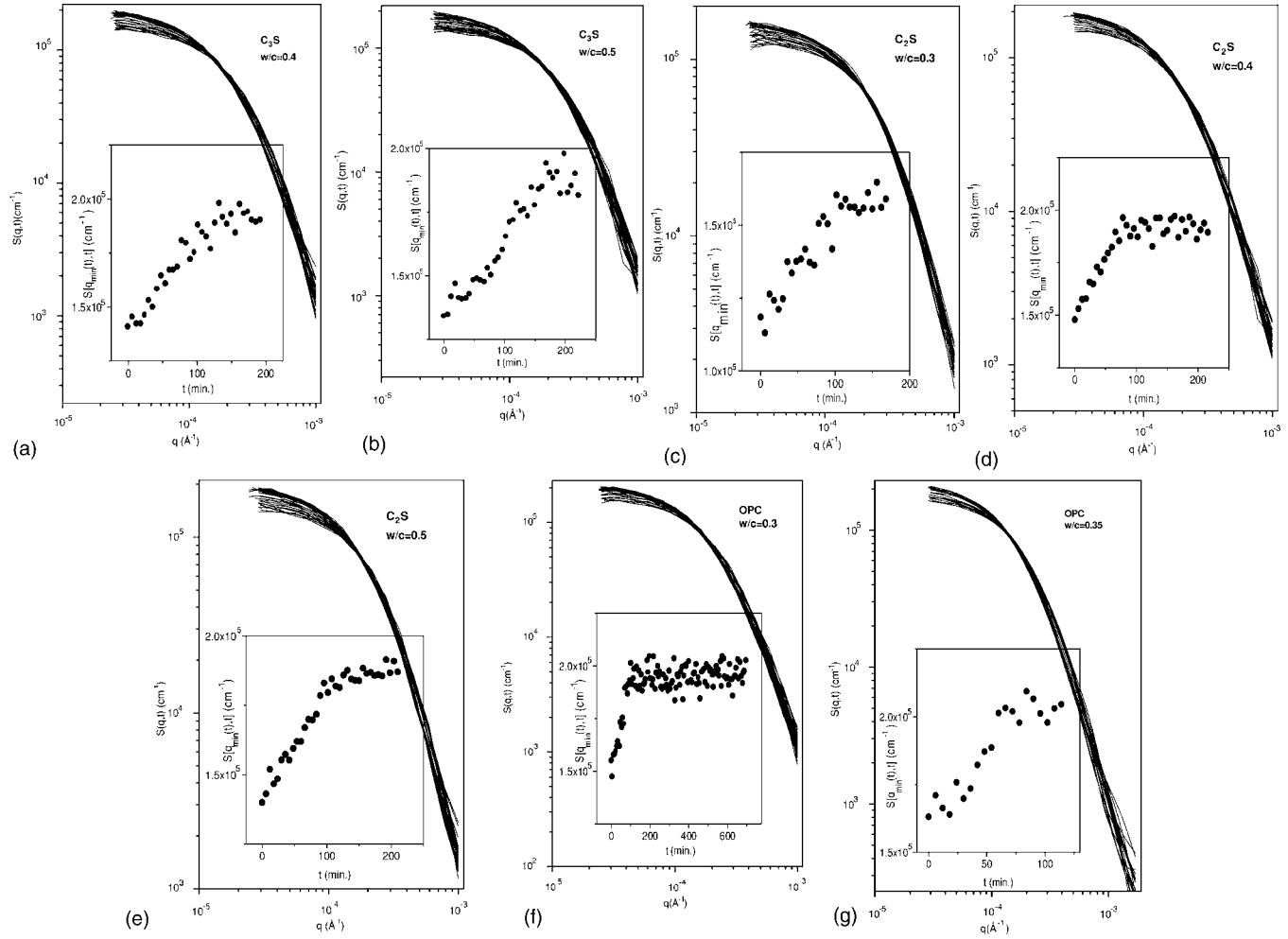

FIG. 1. Time evolution of scattering function $S(q,t)$ for light water hydrating calcium trisilicate (C_3S), calcium disilicate (C_2S), and ordinary portland cement (OPC) with varying w/c ranging from 0.3 to 0.5 by mass. The inset shows the time evolution of $S(q_{\min}(t),t)$ where q_{min} is the lowest attained q value for a particular measurement. q_{min} varies slightly from one measurement to the other and is represented as time dependent.

normalized scattering profiles in the vicinity of $q \to 0$ increases, indicating the growth of the pores. The curvature $\kappa(t)$ of normalized $S(q,t)$ at q is given by

$$\kappa(t) = \frac{|d^2[S(q,t)/S(0,t)]/dq^2|}{(1+\{d[S(q,t)/S(0,t)]/dq\}^2)^{3/2}}. \quad (9)$$

The curvature[62] $\kappa(t)$ in the vicinity of $q \to 0$ of a scattering profile $S(q,t)$ is related to

$$G(t) = -d[\ln[S(q,t)/S(0,t)]]/dq^2 \quad (10)$$

where $G(t)$ is the negative gradient of the Guinier plot of the normalized scattering profile. For a single-scattering profile from a monodisperse population of spheres of radius R, in the vicinity of $q \to 0$, $\kappa = 2R^2/5$ whereas $G = R^2/5$. In subsequent discussions, κ is defined in the vicinity of $q \to 0$ only throughout, if not mentioned otherwise. For a polydisperse population of spherical scatterers, with number density $\rho(R)$ for scatterers of radius R, having the same scattering length density difference, $\kappa = 2\langle R^8 \rangle / 5\langle R^6 \rangle$ where $\langle R^n \rangle$ is the nth moment of the distribution $\rho(R)$. To identify a time-dependent scattering profile from the many shown in Fig. 1, the inset of the figure shows the time evolution of $S(q_{min}(t),t)$ where q_{min} is the lowest attained q value for a particular measurement. q_{min} varies slightly from one measurement to the other and is represented as time dependent.

The time evolution of $\kappa(t)$ for various light-water hydrating specimens is depicted in the inset of Fig. 2. Initially $\kappa(t)$ increases with time and reaches a plateau for light-water hydrating specimens and no systematics have been observed as far as the time at which $\kappa(t)$ reaches the plateau for different time-evolving systems. However, a plateau is reached at relatively later time for OPC specimens. The inset of Fig. 2 also depicts the time evolution of the Porod exponent $\eta(t)$, as estimated from $\ln[S(q,t)]$ vs $\ln(q)$, in the q range $0.000\,25 - 0.001$ Å^{-1} for various hydrating specimens. The Porod exponent $\eta(t)$ for all the light-water hydrating specimens lies in the range of 2–3 indicating the mass fractal natureof the hydrating paste.

Objects exhibiting scale invariance are called fractal objects. Scale invariance implies that the autocorrelation function of the system remains invariant under change of scale up to a multiplicative factor when the scale of observation is changed by some factor b. Hence, $g(br) \sim g(r)$, indicating the validity of dilation symmetry. These kinds of objects are called self-similar under dilation symmetry. This is possible only when $g(r)$ follows a power-law correlation of the form $g(r) \sim r^{-\gamma}$. Mass fractal objects follow a long-range power-law correlation in density, i.e., the mass $M(R)$ within a sphere of radius R is represented as $M(R) \sim R^{D_m}$, where D_m is generally a fractional number and is called the mass fractal dimension of the object. For ramified structures, embedded in a three-dimensional space, the value of D_m lies in the range $1 < D_m < 3$. For a ramified rod and disk, the values of D_m lie in the ranges $0 < D_m < 1$ and $1 < D_m < 2$, respectively. The smaller the value of D_m, the more ramified is the object. Nanoparticles suspended in a liquid, under certain conditions, can aggregate together forming self-similar mass fractal clusters. For example, the structures of porous colloidal aggregates (gold, silica, latex) formed by Brownian motion exhibit dilation symmetry and are well described as mass fractals. For a mass fractal aggregate, the following relation holds good:

$$R = \ell [M(R)]^{1/D_m} \quad (11)$$

where ℓ is termed the lacunarity constant. Lacunarity is a counterpart to the fractal dimension that describes the texture of a fractal. A fractal object having large gaps or holes has high lacunarity; on the other hand, a fractal object having low lacunarity is almost translationally invariant. Fractal objects having the same fractal dimensions can look widely different because of having different lacunarity.

Like mass fractal objects, there are objects with uniform internal density but outer surface exhibiting self-similar geometric properties. Fractal surfaces represent topographical irregularities of the complex surfaces. For a surface fractal object, the surface area $S(R)$ within a circle of radius R is represented as $S(R) \sim R^{D_s}$, where D_s is generally a fractional number lying in the range $2 < D_s < 3$ and is called the surface fractal dimension of the object. Many deposited surfaces produced by a variety of chemical and ballistic procedures are surface fractal in nature. Further, all mass fractal objects are surface fractal in nature invariably, but surface fractal objects need not be mass fractal. In the limit of diffusion-limited aggregation, particles are more likely to adhere to the outer branches of the growing agglomerate rather than penetrate to the core and produce a surface fractal object.

For objects whose volume or mass is fractal such as cluster aggregates, $S(q,t)$ asymptotically approaches the form $S(q,t) \sim q^{-\eta}$ where the exponent η reflects[63] directly the mass fractal dimension D_m. For a mass fractal object, $\eta = D_m$ with $1 < \eta < 3$ and $1 < D_m < 3$. It is evident from the insets of Fig. 2 that the mass fractal dimension of the light-water hydrating gels increases with time of hydration and reaches a plateau after about 150 min with the maximum attained value less than 3. The expected Porod exponent for an ideal smooth surface is 4.

It has been noted that the gross qualitative patterns of the time evolution of κ and η are the same for light-water hydrating specimens and no systematics have been observed as far as the time at which $\kappa(t)$ and $\eta(t)$ reach the plateau for different hydrating specimens with different w/c's. For hydrating OPC specimens, a plateau is reached at relatively later time. The initial increase of D_m with time reflects the transition from a ramified and porous structure to a relatively more compact homogeneous solid matrix by the processes of interlinking and space filling of the disjoint initial gel network with CSH and CH. This observation also explains the increasing compressive strength[64] of hydrated cement with time.

To investigate the extent of validity of the linear theory of phase formation, the time-independent behavior of $\alpha(\mathbf{q})$ $\{=[1/2(t_1 - t_2)]\ln[S(\mathbf{q},t_1)/S(\mathbf{q},t_2)]$ where t_1 and t_2 are the two times of measurements$\}$ has been examined. It has been observed that $\alpha(\mathbf{q})$ does not behave as time independent for any composition of the hydrating mixture even at the

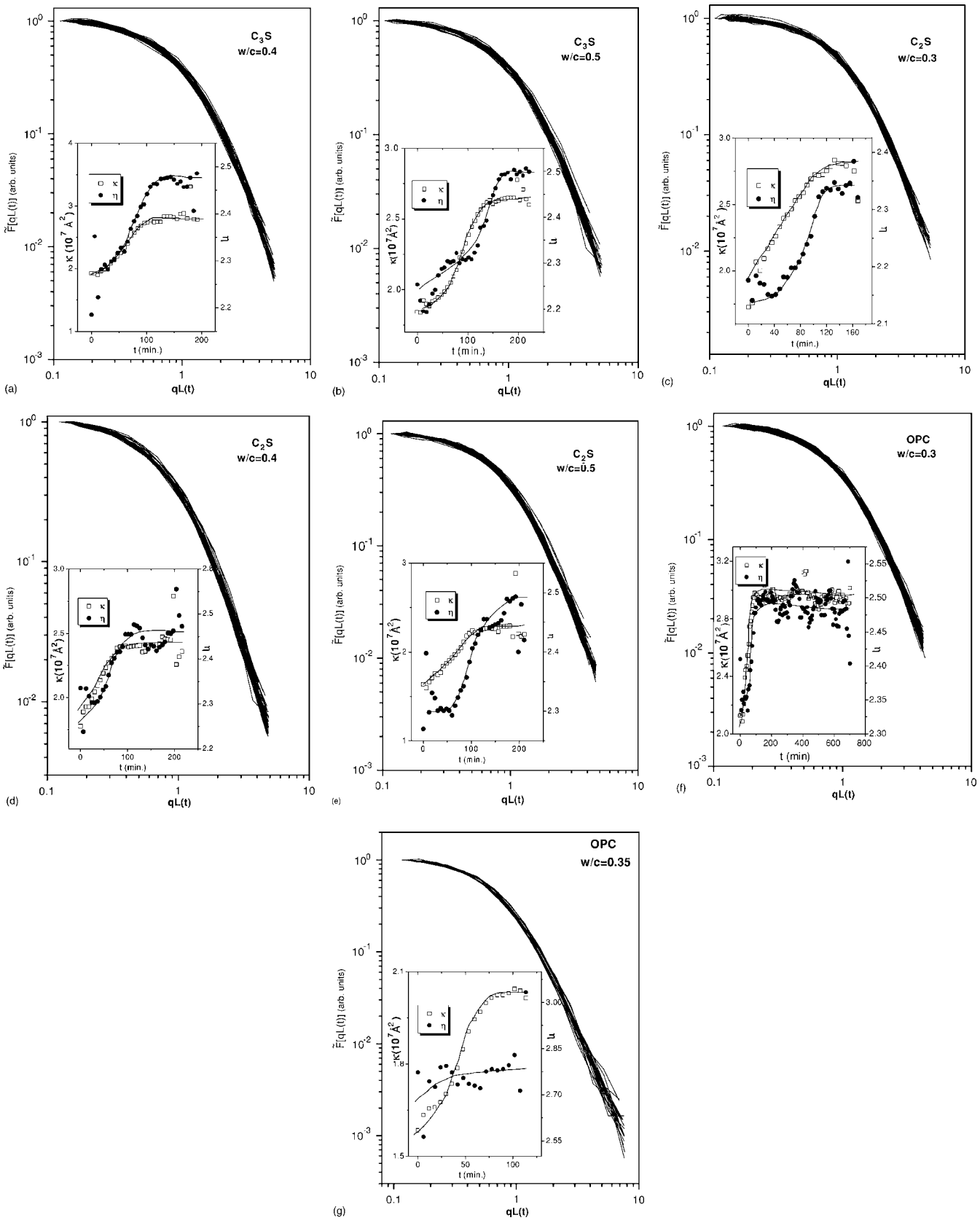

FIG. 2. Scaled scattering function $\tilde{F}(qL(t))$ for light water hydrating C_3S, C_2S, and OPC with varying w/c ranging from 0.3 to 0.5. The inset shows the time evolution of $\kappa(t)$ and $\eta(t)$. The solid lines are only guides to the eye.

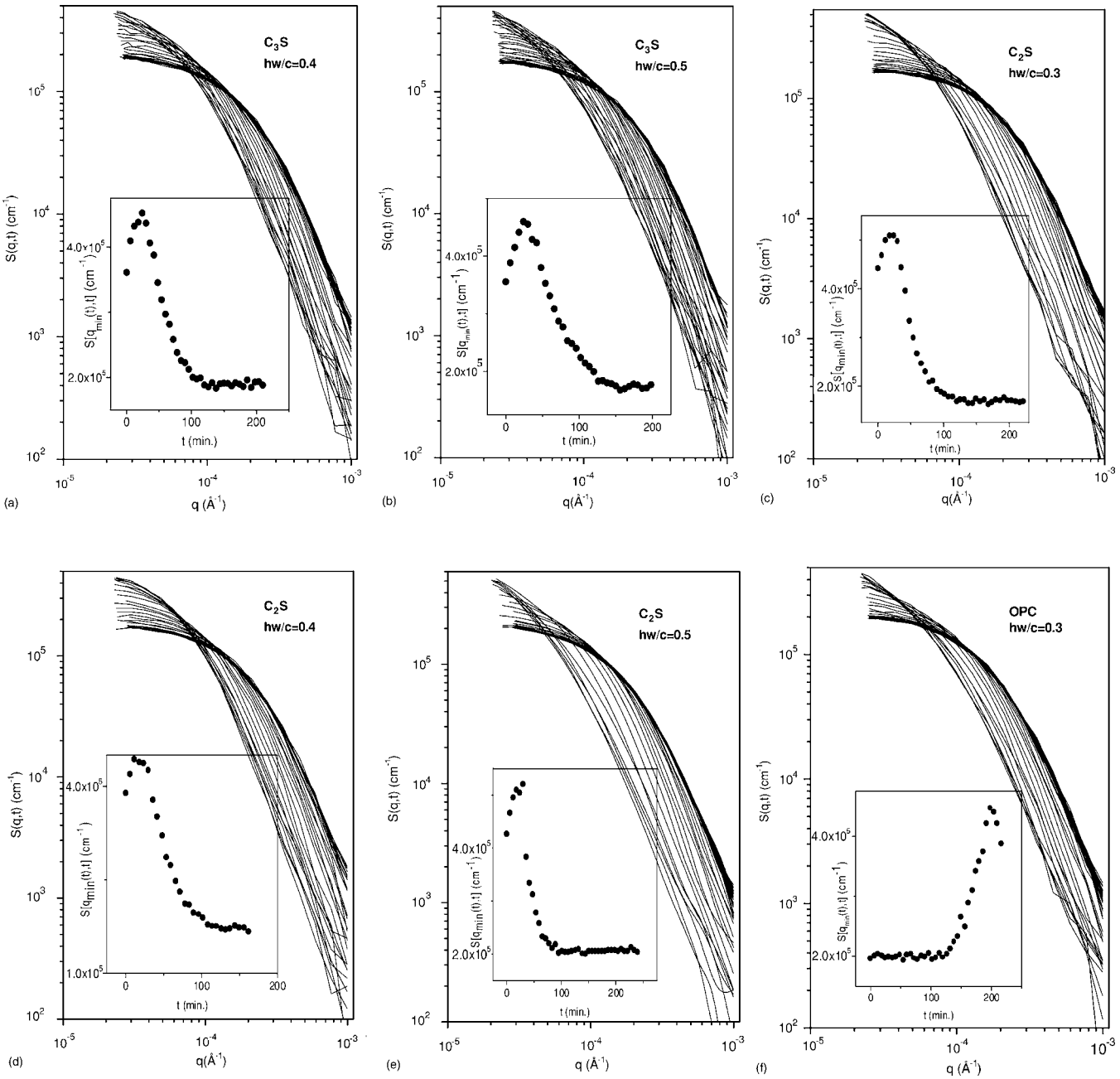

FIG. 3. Time evolution of scattering function $S(q,t)$ for heavy water hydrating C_3S, C_2S, and OPC with varying w/c ranging from 0.3 to 0.5. The inset shows the time evolution of $S(q_{min}(t),t)$ where q_{min} is the lowest attained q value for a particular measurement. q_{min} varies slightly from one measurement to the other and is represented as time dependent.

initial stages of the measurements, indicating the inadequacy of the linear theory to comprehend the observations of the present set of measurements.

The structure factor kinetics in the light of the scaling phenomenon of phase formation has also been examined in the present investigation. The normalized scaling function $\tilde{F}(qL(t))=S(q,t)[L(t)]^{-D_m}/\Sigma q^{D_m}S(q,t)\delta q$ has been calculated, where the characteristic length $L(t)$ has been assumed to be $\sqrt{\kappa}(t)$ and δq is the experimental q increment. It is pertinent to note that for a mass fractal object, the surface area also scales[65] as r^{D_m} for a spherical surface of radius r. Figure 2 depicts the variation of normalized $\tilde{F}(qL(t))$ with dimensionless $qL(t)$ for light-water hydrating calcium disilicate, calcium trisilicate, and OPC with varying w/c's. It is evident from the figures that the normalized scaling functions are time independent, indicating reasonably good agreement with the dynamical scaling hypothesis. Further, the validity of the dynamical scaling phenomenon has not been observed for all the hydrating specimens under investigation for $L(t)=q_1^{-1}(t)$, where $q_1(t)$ is the first moment of the scattering function $S(q,t)$. Further, it is pertinent to note that in the present investigation on hydration of cements, the characteristic length $L(t)$ does not evolve with time according to a power law

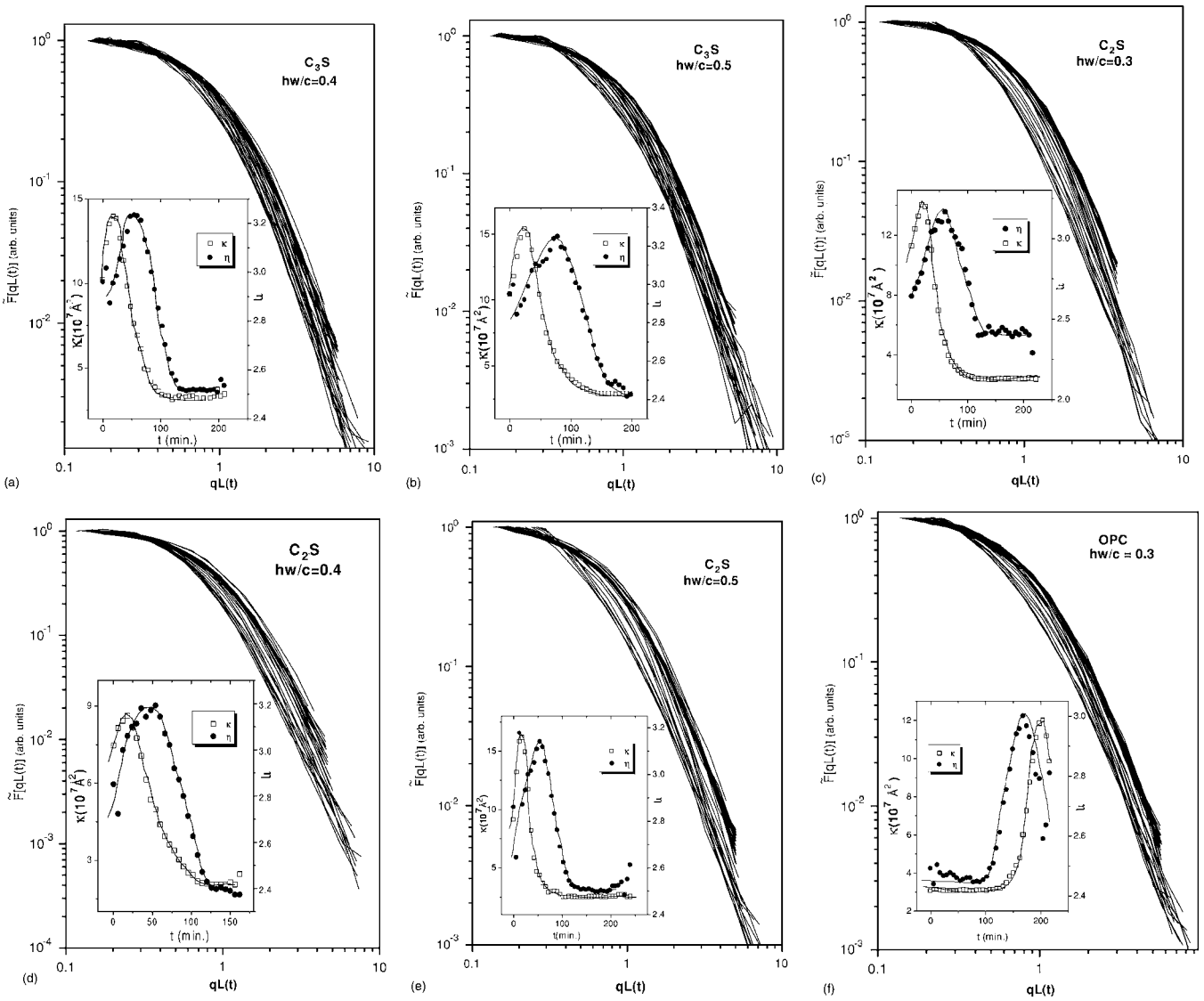

FIG. 4. Scaled scattering function $\tilde{F}(qL(t))$ for heavy water hydrating C_3S, C_2S, and OPC with varying w/c ranging from 0.3 to 0.5. The inset shows the time evolution of $\kappa(t)$ and $\eta(t)$. The solid lines are only guides to the eye.

$$L(t) \propto t^{\beta}. \tag{12}$$

The exponent β is in general model dependent and a wide range of values has been predicted for it. It is known that the elastic effect is responsible for the deviation from the one-third law of Lifshitz and Slyozov.[66] Langer, Bar-on, and Miller[67] obtained $\beta=0.212$ from a time-dependent Ginzburg-Landau model in three dimensions. On the basis of a cluster reaction model, Binder and Stauffer[68] arrived at $\beta=1/(d+2)$ for intermediate temperatures and $\beta=1/(d+3)$ for low temperatures ($T<0.6T_c$), where d is the dimensionality. The value of $\beta=1/(d+2)$ at low temperatures has also been predicted by Furukawa[69] from his analysis of the asymptotic behavior of the kinetic equation. Most of the features predicted have been corroborated well by scattering experiments in binary alloys. For a multicomponent alloy, it has been observed[10,11] that β is temperature dependent and at lower temperature β is not uniform over the entire time range. At higher temperature, the growth of the second phase is driven by the diffusion of atoms while at lower temperature the growth is due to the development of coherence between the clusters. The investigation hinted at the possibility of a nonunique characteristic length. It is to be noted that the theory of Binder and Stauffer[68] predicted a crossover phenomenon where the value of β changes from 1/5 to 1/3.

Since a good agreement with the scaling hypothesis for the case of hydration of silicates with light water has been observed, it was worth considering repeating the experiments with heavy water. The time evolution of the structure factor $S(q,t)$ is depicted in Fig. 3 for heavy water hydrating calcium disilicate, calcium trisilicate, and OPC with varying w/c's ranging from 0.3 to 0.5, respectively. The time evolution of $S(q_{min}(t),t)$ is depicted in the inset of Fig. 3. The inset of Fig. 4 depicts the time evolution of $\kappa(t)$ for various heavy water hydrating specimens. It is evident from the inset of Fig. 4 that with increasing hydration time, the curvature $\kappa(t)$ of the scattering profiles in the vicinity of $q \rightarrow 0$ increases

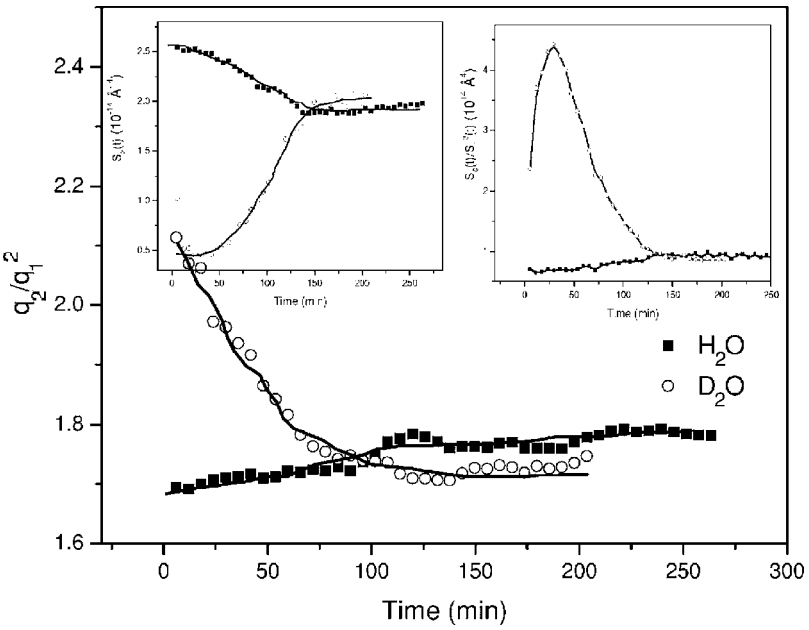

FIG. 5. Time evolution of q_2/q_1^2 for heavy and light water hydrating C_3S with w/c=0.3. Inset 1 shows the time evolution of $S_2(t)$ while inset 2 shows the time evolution of $S_0(t)/S_1^2(t)$. The solid lines are only guides to the eye.

initially, indicating the growth of the inhomogeneities. Subsequently, $\kappa(t)$ and the inhomogeneity size decrease to reach a plateau. This observation is in sharp contrast with the observations in the case of the light water hydrating process. The initial growth of the inhomogeneities persists for about 25 min except for the OPC specimen for which growth continues for about 200 min. The time evolution of the Porod exponent $\eta(t)$, as estimated from $\ln[S(q,t)]$ vs $\ln(q)$ for various hydrating specimens in the q range 0.000 25–0.001 Å^{-1}, is depicted in the insets of Fig. 4. The time-dependent Porod exponents $\eta(t)$ for all the specimens lie in the range of 2–4 indicating the mass fractal nature of the hydrating paste in the beginning. Subsequently, the mass fractal dimension increases, indicating decreasing ramification, resulting finally in a solid core, with increasing hydration time, and a transition from mass fractal to surface fractal occurs. For objects whose surface is fractal such as powders with porous irregular surfaces, the exponent η is related[70] to the surface fractal dimension D_s, where $\eta=6-D_s$ with $3<\eta<4$ and $2<D_s<3$. $\eta(t)$ reaches a maximum and subsequently a further transition from the surface fractal to the mass fractal occurs with time. These results are in contrast to those observed in the case of light water hydrating specimens. But as in hydration of silicates with light water, here too it has been observed that the linear theory of phase formation is inadequate to comprehend the scattering data from hydration of silicates with heavy water.

The validity of the scaling hypothesis has also been examined for the case of hydration of silicates with heavy water. The normalized scaling function $\tilde{F}(qL(t))$ has been estimated with $L(t)=\sqrt{\kappa}(t)$. Variations of $\tilde{F}(qL(t))$ with $qL(t)$ for heavy water hydrating calcium disilicate, calcium trisilicate, and OPC with varying w/c's are depicted in Fig. 4. It is evident from the figure that the normalized scaling functions are not time independent in nature, indicating breakdown of the scaling hypothesis in the case of hydration of silicates with heavy water. Further, it has also been noted that the scaling phenomenon does not hold good for all the hydrating specimens under investigation with $L(t)=q_1^{-1}(t)$ where $q_1(t)$ is the first moment of the structure factor $S(q,t)$. These results are in sharp contrast to those observed in the case of light water hydrating specimens.

The question remains about why scaling is observed in the hydration with light water and not with heavy water. It has been established in the present experiment that in the case of hydration with heavy water, the hydrating mass changes topographically with time, unlike the case of hydration with light water. In the beginning, the hydrating mass is ramified throughout the volume but the degree of ramification decreases as a function of time. Then the mass transforms into objects with uniform internal density of the unramified core but outer surface structure exhibiting self-similar geometric properties and of ramified nature. But further on, the ramified surface grows into a ramified volume and the degree of ramification increases with time. This topographical change of the hydrating mass as a function of time could be one of the plausible reasons why scaling is not observed in the case of hydration with heavy water. In fact, we have not come across any scattering experiment where scaling has been observed despite the topographical change of the second phase with time. We are unable to put forward a more conclusive reason at this stage.

A consequence of the scaling hypothesis is that the unnormalized nth moment of the structure factor behaves as

$$S_n(t) = \int q^n S(q,t)dq = L^{2-n}(t) \int [qL(t)]^n F(qL(t))d[qL(t)] \tag{13}$$

and

$$q_n(t) \equiv S_n(t)/S_0(t) \propto L^{-n}(t). \tag{14}$$

It is prudent to examine the extent of validity of the scaling hypothesis, manifested through Eqs. (13) and (14), experi-

mentally since accurate measurement of the structure factor is possible only over a restricted range of wave vector. The long-wavelength cutoff in the structure factor introduces errors in the lower moments, particularly at later times, whereas the short-wavelength cutoff affects the higher-order moments. It has been observed (Fig. 5) that the ratio q_2/q_1^2 is slowly varying with time for light water hydrated specimen compared with the heavy water hydrated specimen of calcium trisilicate with w/c=0.3. The fact that the measured integrated intensity $S_2(t)$, proportional to the volume fraction of the new phase, is time dependent and is therefore responsible for the stronger time dependence of the ratio $S_0(t)/S_1^2(t)$. Figure 5 depicts the variation of $S_2(t)$ with time for the hydrating specimens of C_3S with w/c=0.3. The time dependence of the moment ratios is much stronger, as evident from Fig. 5, for heavy water hydrating specimens compared to the light water hydrating specimens. Scattering data for light water and heavy water hydrating C_3S with w/c=0.3 are available in the literature.[71]

IV. CONCLUSIONS

In the present work, an attempt has been made to establish the hydration kinetics of silicates with light and heavy water. It is shown that the kinetics are of nonlinear nature even at the initial time. The scattering data could not be interpreted in terms of a linear theory based on the diffusion equation. It has also been demonstrated that light water hydration of silicates exhibits a scaling phenomenon for a characteristic length with a different measure. In the present work, observation of the exhibition of the scaling phenomenon for a non-Euclidean system has been reported. The temporal behavior of the characteristic length has been observed to be far from a power law. The second phase appears to grow initially with time in the case of light water hydrated specimens. Subsequently, the domain size of the second phase saturates. As far as chemistry is concerned, the hydration of silicates with light and heavy water is expected to be quite similar except for kinetics. However, some contrasting behavior has been observed in the case of hydration of silicates with heavy water as far as the kinetics of new phase formation is concerned compared with the behavior in the case of light water hydration. The domain size grows in the beginning for a very short time and subsequently appears to shrink with time, reaching saturation ultimately. The scaling phenomenon, with all possible measures of the characteristic length, has not been established for the hydration kinetics with heavy water. The topographical change of the hydrating mass as a function of time could be the plausible reason why scaling is not observed in the case of hydration with heavy water. We are unable to put forward a more conclusive reason at this stage. The present experiment indicates that the phenomenon of dynamical scaling should be brought into closer scrutiny for many more systems in the future. To the best of our knowledge, investigations examining behavior of the scaling laws under confined geometry and under random field have not been touched upon so far. Investigations on these lines are strongly recommended in the future.

ACKNOWLEDGMENTS

We gratefully acknowledge the kind support and keen interest of several colleagues of ours in this work. This work has been carried out with the association EURATOM-OEAW.

*Corresponding author. Email address: smazu@apsara.barc.ernet.in

[1] M. Hennion, D. Ronzaud, and P. Guyot, Acta Metall. **30**, 599 (1982).
[2] S. Komura, K. Osamura, H. Fujii, and T. Takeda, Phys. Rev. B **30**, 2944 (1984).
[3] S. Katano and M. Iizumi, Phys. Rev. Lett. **52**, 835 (1984).
[4] S. Komura, K. Osamura, H. Fujii, and T. Takeda, Phys. Rev. B **31**, 1278 (1985).
[5] M. Furusaka, Y. Ishikawa, and M. Mera, Phys. Rev. Lett. **54**, 2611 (1985).
[6] O. Lyon and J. P. Simon, Phys. Rev. B **35**, 5164 (1987).
[7] B. Rodmacq, M. Maret, J. Laugier, L. Billard, and A. Chamberod, Phys. Rev. B **38**, 1105 (1988).
[8] R. D. Lorentz, A. Bienenstock, and T. I. Morrison, Phys. Rev. B **49**, 3172 (1994).
[9] M. J. Regan and A. Bienenstock, Phys. Rev. B **51**, 12170 (1995).
[10] S. Mazumder, D. Sen, I. S. Batra, R. Tewari, G. K. Dey, S. Banerjee, A. Sequeira, H. Amenitsch, and S. Bernstorff, Phys. Rev. B **60**, 822 (1999).
[11] R. Tewari, S. Mazumder, I. S. Batra, G. K. Dey, and S. Banerjee, Acta Metall. **48**, 1187 (2000).
[12] D. Sen, S. Mazumder, R. Tewari, P. K. De, H. Amenitsch, and S. Bernstorff, J. Alloys Compd. **308**, 250 (2000).
[13] A. Chakrabarti, R. Toral, J. D. Gunton, and M. Muthukumar, Phys. Rev. Lett. **63**, 2072 (1989).
[14] B. Dunweg and K. Kremer, Phys. Rev. Lett. **66**, 2996 (1991).
[15] M. Takenaka and T. Hashimoto, Phys. Rev. E **48**, R647 (1993).
[16] G. Brown and A. Chakrabarti, Phys. Rev. E **48**, 3705 (1993).
[17] G. Krausch, C. A. Dai, E. J. Kramer, and F. S. Bates, Phys. Rev. Lett. **71**, 3669 (1993).
[18] M. Rubinstein, R. H. Colby, and A. V. Dobrynin, Phys. Rev. Lett. **73**, 2776 (1994).
[19] W. R. White and P. Wiltzius, Phys. Rev. Lett. **75**, 3012 (1995).
[20] S. R. Shannon and T. C. Choy, Phys. Rev. Lett. **79**, 1455 (1997).
[21] P. W. Zhu, J. W. White, and J. E. Epperson, Phys. Rev. E **62**, 8234 (2000).
[22] E. Falck, O. Punkkinen, I. Vattulainen, and T. Ala-Nissila, Phys. Rev. E **68**, 050102(R) (2003).
[23] C. O. Kim and W. L. Johnson, Phys. Rev. B **23**, 143 (1981).
[24] A. F. Craievich and J. M. Sanchez, Phys. Rev. Lett. **47**, 1308 (1981).
[25] A. F. Craievich, J. M. Sanchez, and C. E. Williams, Phys. Rev. B **34**, 2762 (1986).
[26] S. Sen and J. F. Stebbins, Phys. Rev. B **50**, 822 (1994).
[27] A. Wiedenmann and Jun-Ming Liu, Solid State Commun. **100**, 331 (1996).

[28] A. Malik, A. R. Sandy, L. B. Lurio, G. B. Stephenson, S. G. J. Mochrie, I. McNulty, and M. Sutton, Phys. Rev. Lett. **81**, 5832 (1998).
[29] J. H. He and E. Ma, Phys. Rev. B **64**, 144206 (2001).
[30] A. Chakrabarti, Phys. Rev. Lett. **69**, 1548 (1992).
[31] J. C. Lee, Phys. Rev. B **46**, 8648 (1992).
[32] C. K. Chan, Phys. Rev. Lett. **72**, 2915 (1994).
[33] J. Jacob, A. Kumar, S. Asokan, D. Sen, R. Chitra, and S. Mazumder, Chem. Phys. Lett. **304**, 180 (1999).
[34] C. M. Knobler and N. C. Wong, J. Phys. Chem. **85**, 1972 (1981).
[35] Y. C. Chou and W. I. Goldburg, Phys. Rev. A **23**, 858 (1981).
[36] D. N. Sinha and J. K. Hoffer, Physica B & C **107**, 155 (1981).
[37] S. Bastea and J. L. Lebowitz, Phys. Rev. Lett. **78**, 3499 (1997).
[38] M. Kriechbaum, G. Degovics, J. Tritthart, and P. Laggner, Prog. Colloid Polym. Sci. **79**, 101 (1989).
[39] A. Heinemann, H. Hermann, K. Wetzig, F. Haeussler, H. Baumbach, and M. Kroening, J. Mater. Sci. Lett. **18**, 1413 (1999).
[40] R. A. Livingston, D. A. Neumann, A. J. Allen, S. A. Fitzgerald, and R. Berliner, Neutron News **11** (4), 18 (2000).
[41] C. V. Santilli, S. H. Pulcinelli, and A. F. Craievich, Phys. Rev. B **51**, 8801 (1995).
[42] J. Marro, J. L. Lebowitz, and M. H. Kalos, Phys. Rev. Lett. **43**, 282 (1979).
[43] J. L. Lebowitz, J. Marro, and M. H. Kalos, Acta Metall. **30**, 297 (1982).
[44] H. Toyoki, Phys. Rev. A **42**, 911 (1990).
[45] A. J. Bray and S. Puri, Phys. Rev. Lett. **67**, 2670 (1991).
[46] F. Liu and G. F. Mazenko, Phys. Rev. B **45**, 6989 (1992).
[47] A. J. Bray, Adv. Phys. **43**, 357 (1994).
[48] J. W. Cahn, Acta Metall. **9**, 795 (1961).
[49] A. J. Bray and K. Humayun, J. Phys. A **23**, 5897 (1990); A. J. Bray, K. Humayun, and T. J. Newman, Phys. Rev. B **43**, 3699 (1991).
[50] P. Fratzl and J. L. Lebowitz, Acta Metall. **37**, 3245 (1989).
[51] P. Fratzl, J. Appl. Crystallogr. **24**, 593 (1991).
[52] F. Langmayr, P. Fratzl, and G. Vogl, Acta Metall. Mater. **40**, 3381 (1992).
[53] A. Coniglio and M. Zannetti, Europhys. Lett. **10**, 575 (1989).
[54] A. J. Bray, Phys. Rev. Lett. **62**, 2841 (1989); A. J. Bray, Phys. Rev. B **41**, 6724 (1990).
[55] E. Velasco and S. Toxvaerd, Phys. Rev. Lett. **71**, 388 (1993).
[56] A. P. Y. Wong, P. Wiltzius, and B. Yurke, Phys. Rev. Lett. **68**, 3583 (1992).
[57] A. P. Y. Wong, P. Wiltzius, R. G. Larson, and B. Yurke, Phys. Rev. E **47**, 2683 (1993).
[58] M. Rao and A. Chakrabarti, Phys. Rev. E **49**, 3727 (1994).
[59] S. Mazumder, D. Sen, T. Saravanan, and P. R. Vijayaraghavan, J. Neutron Res. **9**, 39 (2001).
[60] M. Hainbuchner, M. Villa, G. Kroupa, G. Bruckner, M. Baron, H. Amenitsch, E. Seidl, and H. Rauch, J. Appl. Crystallogr. **33**, 851 (2000).
[61] U. Bonse and M. Hart, Appl. Phys. Lett. **7**, 238 (1965).
[62] S. Mazumder, D. Sen, S. K. Roy, M. Hainbuchner, M. Baron, and H. Rauch, J. Phys.: Condens. Matter **13**, 5089 (2001).
[63] T. Freltoft, J. K. Kjems, and S. K. Sinha, Phys. Rev. B **33**, 269 (1986).
[64] P. Pfeifer and D. Avnir, J. Chem. Phys. **79**, 3558 (1983); P. Pfeifer and D. Avnir, J. Chem. Phys. **80**, 4573(E) (1984).
[65] R. B. Williamson, Prog. Mater. Sci. **15**, 189 (1972).
[66] I. M. Lifshiftz and V. Slyozov, J. Phys. Chem. Solids **19**, 35 (1961).
[67] S. Langer, M. Bar-on, and H. D. Miller, Phys. Rev. A **11**, 1417 (1975).
[68] K. Binder and D. Stauffer, Phys. Rev. Lett. **33**, 1006 (1974).
[69] H. Furukawa, Phys. Rev. A **23**, 1535 (1981).
[70] D. F. R. Mildner and P. L. Hall, J. Phys. D **19**, 1535 (1986).
[71] S. Mazumder, D. Sen, A. K. Patra, S. A. Khadilkar, R. M. Cursetji, R. Loidl, M. Baron, and H. Rauch, Phys. Rev. Lett. **93**, 255704 (2004).